Int. J. Electrochem. Sci., 11 **(2016)** 6064 – 6077, doi: 10.20964/2016.07.19

International Journal of
ELECTROCHEMICAL
SCIENCE
www.electrochemsci.org

Quasi-solid-state Electrolyte for Dye Sensitized Solar Cells Based on Nanofiber PMA-PVDF and PMA-PVDF / PEG Membranes

Marwa Fathy[1,*], *Jehan El Nady*[1], *Mamoun Muhammed*[2], *Shaker Ebrahim*[3], *Moataz B. Soliman*[3], *Abd El-Hady B. Kashyout*[1]

[1] Electronic Materials Department, Advanced Technology and New Materials Research Institute, City of Scientific Research and Technological Applications (SRTA-City), New Borg El-Arab City, P.O. Box 21934, Alexandria, Egypt.
[2] Division of Functional Materials, KTH- Royal Institute of Technology, SE-10044 Stockholm, Sweden.
[3] Materials Science Department, Institute of Graduate Studies and Research, Alexandria University, 163 Horrya Avenue, P.O. Box 832, Shatby, 21526 Alexandria, Egypt.
[*]E-mail: mfathy@mucsat.sci.eg

Received: 27 March 2016 / *Accepted:* 17 April 2016 / *Published:* 4 June 2016

Novel electrospun membranes quasi-solid electrolytes based on blends of polymethylacrylate (PMA) - polyvinylidene fluoride (PVDF), and PMA-PVDF/PEG (polyethylene glycol) are prepared by electrospinning technique and applied as quasi-solid state electrolytes in dye sensitized solar cells (DSSCs). The membranes are characterized by Fourier transform infrared (FT-IR) spectrophotometer, differential scanning calorimeter (DSC), Scanning electron microscopy (SEM), and Electrochemical impedance spectroscopy. The crystallinity obtained from the DSC data increased with the increase of PVDF wt% in PMA-PVDF blend and then decreased for the PMA-PVDF/PEG membranes. The fully interconnected porous structure of the host polymer membranes of PMA-PVDF (4:6 wt%) exhibited a high electrolyte uptake reached to ~ 265% and an ionic conductivity of 2.1×10^{-3} S cm^{-1}, which is increased to 406.3%, and 3.2×10^{-3} S cm^{-1}, respectively for PMA-PVDF/PEG (4:6:4 wt%) membrane. DSSC is assembled by PMA-PVDF(4:6 wt%) and attained an overall energy conversion efficiency of 6.6% at light intensity of 100 mW cm^{-2}. The presence of 4 w% PEG in the electrolyte membrane increased the energy conversion efficiency to 7 % giving a promise candidate for scaling up this type of DSSCs.

Keywords: Dye sensitized solar cells, quasi solid electrolyte, electrospinning, ionic conductivity.

1. INTRODUCTION

Dye-sensitized solar cells (DSSCs) using organic liquid electrolytes have attracted considerable attention owing to its potential for low cost power production as well as a portable energy supply.[1]

DSSCs based on liquid electrolytes (The most commonly used redox couple is iodide/tri-iodide (I^-/I_3^-) in an organic liquid electrolyte) have already achieved high conversion efficiencies of 14%.[1,2]

The liquid electrolyte is highly corrosive, volatile and photoreactive, interacting with common metallic components and sealing materials.[3] The ultimate solutions would be purely solid-state cells, given the inevitable problems of any liquid electrolyte, such as leakage, heavy weight and complex chemistry. In recent years, researchers have developed several types of hole-transporting materials (HTMs) to replace iodine-based liquid electrolytes.[4] In 2004, Kumara et al. used CuI as the HTM and Ru complex dye N3 as the sensitizer and the highest efficiency for inorganic HTM-based DSSCs is reported to be 4.7% because the mobility is very low.[5] Gratzel et al. 1998, and 2011[6-7] fabricated solar cells using spiro-OMeTAD (TAD is 2,2',7,7'-tetranis(N,N-di-p-methoxyphenyl-amine)9,9'-spirobifluorene), and bis-EDOT (EDOT is 2,2'-bis(3,4-ethylenedioxythiophene) exhibit the highest conversion efficiencies among organic and conducting polymer materials of 6.08% and 6.1%, respectively. The problem of solid HTMs in DSCs is poor filling of the nanoporous TiO_2 layer; this interrupts the hole-conducting path between the HTM and the dye molecule adsorbed on TiO_2.[3,8] To overcome this problem is to use a gel electrolyte or better known as quasi-solid electrolyte.[9] Gel electrolytes have higher ionic conductivity than solid polymer electrolytes due to the presence of trapped liquids in the polymer matrix and the gel electrolytes flexibility enables them to make good contact with the photoelectrode and counter electrode.[9]

Lan et al. 2006;[10] Wu et al. 2006;[11] Ileperuma et al. 2011;[12] Xiang et al. 2011;[13] are used poly(acrylic acid)/gelation/polyaniline (overall energy conversion efficiency of light-to-electricity of 2.75% under irradiation of 60 mW cm^{-2}),[10] poly(acrylamide) (3% under irradiation of 60 mW cm^{-2},[11] polyacrylonitrile (PAN) (7%),[12] poly(vinyl pyridine-co-acrylic nitrile) (6.1%),[13] respectively. The electrochemical impedance spectroscopy of polymer-gelled DSSCs also indicated less resistance associated with the Nernstian diffusion within the electrolytes as the polymer of lower T_g was adopted by Lin et al. in 2008. The power efficiency of PMA-gelled DSSC is reached to 7.17%.[14]

Electrospinning technique is very promising, versatile,[15] simple, and cost-effective approach for producing polymeric and inorganic nanofibers with structures that vary with the processing parameters.[16] In 2008, Kim et al.[17] fabricated quasi-solid-state solar cells with the electrospun PVdF-HFP membrane electrolyte with 7.3% efficiency. This efficiency is slightly lower than the value of 7.8% observed for the solar cells with the conventional liquid electrolyte (illumination intensity of 100 mW cm^{-2}). But, the electrospun PVdF-HFP membrane encapsulated the electrolyte solution well without leakage and displayed better long-term stability than that with conventional liquid electrolyte.[17]

In our previous work, nanofibers PMA membrane was used as based quasi solid electrolyte and 1.4% incident- to-photon conversion efficiency was obtained. The low cell efficiency problem is the

elasticity of PMA polymer lead to the formation of fibers network and membrane shrink with time which reduces the ions mobility and cell efficiency.[18] PVDF with its high mechanical stability and chemical inertness blended with PMA can be used to avoid the shrinkage of PMA.[19] Also, the presence of fluorine atom in PVDF which has the smallest ionic radius and the largest electronegativity, is expected to improve the ionic transport and reduce the recombination rate at semiconductor/ polymer electrolyte interface in DSSC.[20]

Here, we report a new type of quasi-solid-state solar cell system that consists of the quasi PMA-PVDF nanofibers membrane based electrolyte and n-type nanoporous TiO_2 with the dye N719 (cis-diisothiocyanato-bis(2,2'-bipyridyl-4,4'-dicaboxylato) ruthenium(II) bis-(tetrabutylammonium)). The incident photon-to-current conversion efficiency (IPCE) measurements of our cells exhibit 6.6%. In order to decrease the T_g and enhance the ionic conductivity of the quasi solid electrolyte, PMA-PVDF/PEG (with its high polarity) nanofibers membrane was prepared. It was noted that, the performance of DSCs was improved to 7% for cell area of 1 cm^2 and illumination intensity of 100 mW cm^{-2}.

2. EXPERIMENTAL

2.1. Materials

Methyl acrylate, PVDF (Mwt of 534.000), PEG (Mw of 400), N,N-dimethylformamide (DMF, 99.5%) and acetone (Ac) 99.5% were obtained from (Riedel-de Haen.) Potassium persulfate (KPS), iodine (I_2), lithium iodide (LiI), 4-tert-butylpyridine (TBP), and 3-methoxyproponitrile were purchased from (Sigma-Aldrich Co.) All the materials were used as-received without further treatment. PMA, Indium-doped SnO_2-layered (ITO) glass (15 Ω/sq, T= 85-95%), nanoparticles TiO_2 (Anatase with avg. diameter of 8-9 nm), and Pt counter electrode on ITO glass substrates were prepared as reported in our previous work.[21-22] N719 dye $[(C_4H_9)_4N]_2[Ru(II)L_2(NCS)_2]$, where L is 2,2′-bipyridyl-4,4′-dicarboxylic acid, rutheniumTBA535 get from Solaronix.

2.2. Preparation of PMA-PVDF, and PMA-PVDF/PEG nanofiber membranes

Electrospun membranes of PMA-PVDF blend with different weight ratios (S1 to S4) in a mixture of acetone/N,N-dimethylformamide (DMF) (6:4 v/v) were prepared at 20 kV applied voltage and tip to collector distance of 15 cm as presented in Table 1.

The polymer solutions were placed in a 10 mL syringe equipped with stainless steel gauge needle. The needle was connected to a high-voltage power supply (HV HiPotronics). The solution was constantly and continuously supplied using a syringe pump (Harvard Apparatus, Syringe infusion pump 22) with a mass flow rate of 0.5 ml/h. The nanofibers membranes were dried in vacuum oven at 70 ˚C for 12 h to remove any remaining solvent.

For PMA-PVDF/PEG blend nanofiber membranes using different PEG weight ratios (S5 to S7) were prepared with the same electrospinning parameters. All experiments were carried out at room temperature.

Table 1. Different conditions used to optimize the electrospun nanofibers.

Sample code	Membrane composition [wt%]		Applied voltage [kV]	Feed rate [mL/h]	TCD [cm]	Solvent Ac:DMF [v/v]
S1	PMA-PVDF	9:1	20	0.5	15	6:4
S2		6:4				
S3		4:6				
S4		3:7				
S5	PMA-	4:6:2				
S6	PVDF/PEG	4:6:4				
S7		4:6:8				

2.2.1. Characterization of nanofiber membranes

The morphology of the electrospun membranes was observed by scanning electron microscope (JEOL, JSM-6360 LA). The structure analysis was carried out using X-Ray diffractometer (Schimadzu 7000, Japan) and Fourier transform infrared spectroscopy (Shimadzu FTIR- 8400 S, Japan). Membranes thermal properties were investigated using a differential scanning calorimeter (DSC- 60 Schimadzu, Japan) and the degree of crystallinity (χ_c) of the sample was determined from DSC curve using Equation 1:[23]

$$\chi_c = \left({\Delta H_f}/{\Delta H_f^*} \right) \times 100\% \quad (1)$$

where ΔH_f and ΔH_f^* are melting enthalpies of the present sample and of perfectly crystalline PVDF, respectively. In this study, a value of 104.7 J g^{-1} is used for ΔH_f^*.

The electrolyte uptake of polymer membrane is calculated according to the following Equation 2:[24]

$$Uptake\ (\%) = \left({(W_i - W_0)}/{W_0} \right) \times 100 \quad (2)$$

where W_i andW_0 are the weight of the wet (after soaking in the liquid electrolyte) and dry membranes, respectively. The porosity (*P*) is determined by immersing the dry membrane in n-butanol for 1 h. Equation 3 is used to calculate *P*:[25]

$$P(\%) = \frac{\left({M_{BuOH}}/{\rho_{BuOH}} \right)}{\left(\left[{M_{BuOH}}/{\rho_{BuOH}} \right] + \left[{M_m}/{\rho_P} \right] \right)} \times 100 \quad (3)$$

where M_m is the mass of the dry membrane, M_{BuOH} is the mass of n-butanol absorbed, ρ_{BuOH} and ρ_P are the densities of n-butanol and polymer, respectively.[26]

The ionic conductivity (σ) of the electrospun membranes was measured from alternating current (AC) impedance test using electrochemical impedance analyzer (Gamry

Potentiostat/Golvannostat G750). The blocking cell of copper/membrane/copper was used at frequency range from 10 Hz to 100 kHz at AC amplitude of 5 mV. Thus, the ionic conductivity (σ) could be calculated from the following Equation 4:[27]

$$\sigma = {}^{d}/_{R_b S} \qquad (4)$$

where, R_b is the bulk resistance which taken at the intercept of the Nyquist plot with the real axis, d is the polymer membrane thickness, and S is the area of the symmetrical electrode.

2.3. Fabrication of quasi-solid state DSSC

A thin layer of nonporous TiO_2 film (thickness about 10 μm) was obtained by spreading titania paste on ITO glass substrate using doctor blade technique.[22] The film was dried at 70 °C for 10 min and then annealed at 450 °C for 30 min. The TiO_2 photoelectrode was sensitized by immersing it in ethanolic solution of N719 dye (0.5 mM) for 24 hrs at room temperature. TiO_2 electrode was rinsed with anhydrous ethanol and dried in moisture free air. The counter electrode was prepared by deposited Pt layer (thickness 1.75μm) on ITO glass substrate using RF-sputtering technique followed by annealing on air at 450 °C for 45 min.

Quasi-solid state DSSCs using electrospun membranes samples were fabricated by sandwiching a slice of the electrospun membrane (thickness 30μm) between photoanode and a Pt counter electrode. A drop of the electrolyte solution [LiI (0.5 M), I_2 (0.05 M), and 4-*tert*-butylpyridine (0.5 M) in 3-methoxyproponitrile)] was introduced into the clamped electrodes. The active area of DSSC was 1 cm^2.

2.3.1. Cell characterization

The photocurrent density-voltage (J-V) curve of the assembled DSSCs was measured by Solar Simulator (PET Photo Emission Tech., Inc. USA). A Xenon lamp with an AM 1.5 filter (Oriel) was used to illuminate the DSSCs at 100 mW cm^{-2}.

The photoelectrochemical parameters, i.e., the fill factor (FF) and light-to-electricity conversion efficiency (η), were calculated by the following two Equations 5 and 6:[28]

$$FF = \left({}^{(V_{max}J_{max})}/_{(V_{oc}J_{sc})} \right) \qquad (5)$$

$$\eta(\%) = \left((V_{max}J_{max})/P_{in} \right) \times 100 = \left({}^{(V_{oc}J_{sc}FF)}/_{P_{in}} \right) \times 100 \qquad (6)$$

where J_{sc} is the short-circuit current density (mA cm^{-2}), V_{oc} is the open-circuit voltage (V), and P_{in} is the incident light power (mW cm^{-2}). J_{max} (mA cm^{-2}) and V_{max} (V) are the current density and voltage in the J-V curve, respectively, at the point of maximum power output.

3. RESULTS & DISCUSSION

3.1. FTIR analysis

FTIR analysis was employed to investigate the interaction between the polymers matrix. Fig. 1 shows the FTIR spectra of the as-prepared electrospun membranes for the samples shown in Table 1 (S1 – S7). Poly methylacrylate has an absorption peak at 1720 cm^{-1} corresponding to the carbonyl group (C=O).[29] Strong peaks at 840, 511, and 470 cm^{-1} are characteristic peaks of β-PVDF.[30] For PMA-PVDF blends, the peak of (CF_2) is observed and the intensity of the carbonyl group is decreased with gradually increase the wt% ratio of PVDF in the blends of samples S1, S2, S3, and S4. FTIR results indicate the possible interactions between carbonyl group of PMA and CH_2 group of PVDF which indicate the formation of the blends.[31] With the addition of PEG to the PMA-PVDF blend with 2 wt% ratio of 4:6 (S5, S6, and S7), the carbonyl band appears at same wave number, but with a lower intensity, indicating interaction with the PEG forming weak hydrogen bond as shown below;[32-33]

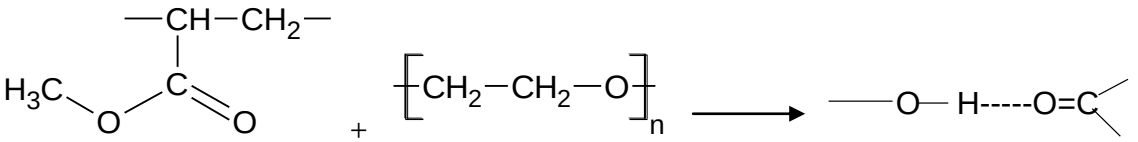

PMA PEG Bond between PMA and PEG

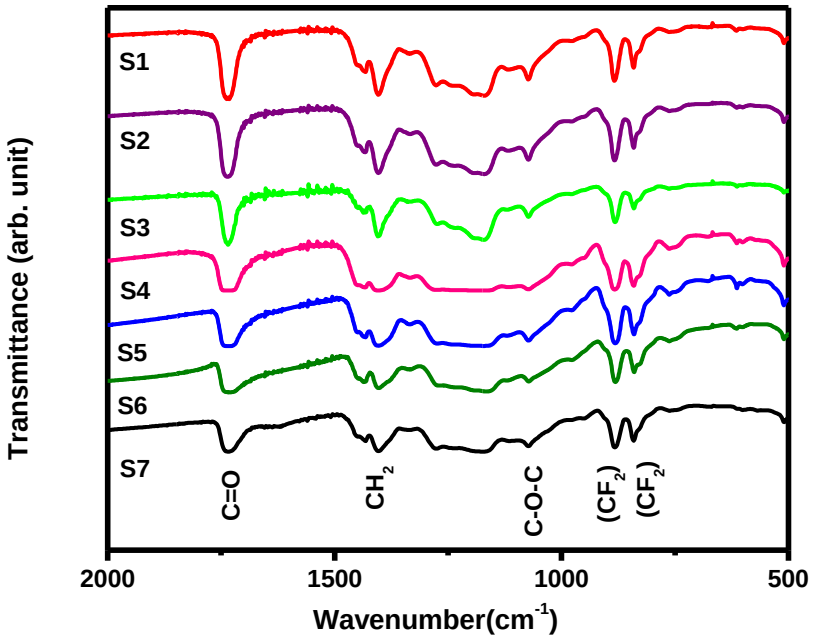

Figure 1. FTIR spectra of electrospun PMA-PVDF and PMA-PVDF/PEG nanofiber membranes.

3.2. Thermal analysis

The effect of incorporation of PVDF and PEG with different weight ratios on the thermal properties of electrospun nanofiber membranes (PMA and PMA-PVDF, respectively) such as glass transition temperature (T_g) as the inflection point, melting temperature (T_m) as the peak of the melting endotherm, and melting enthalpy is investigated by means of DSC.[34] Also, the degree of crystallinity (χ_c) of the sample is determined from DSC curve (as shown in Fig. 2) and calculated using Equation (2). The values of T_g, T_m, melting enthalpy and degree of crystallinity of all samples were presented in Table 2. The degree of crystallinity of electrospun PMA-PVDF blend increase from 4.04% to 31.3% as the PVDF weight content increased from 1 to 7 wt% due to improve the crystallinity of the blend by the interaction between the crystalline PVDF and fully amorphous PMA polymer which also lead to increase the melting enthalpy.

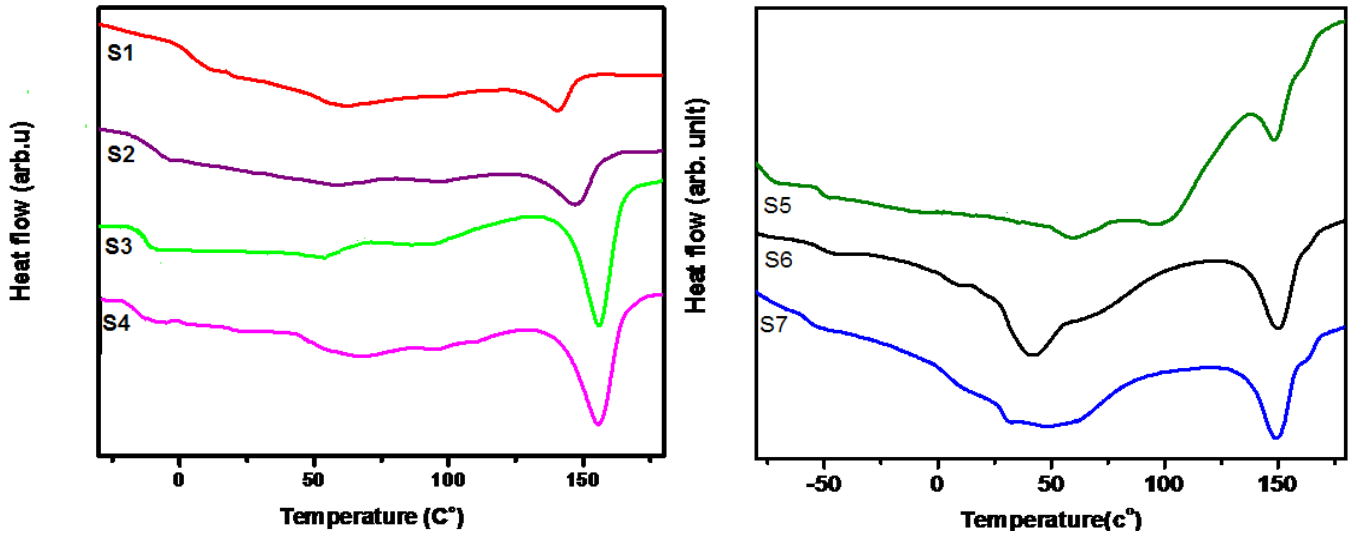

(a) (b)

Figure 2. DSC thermograms of electrospun (a) PMA-PVDF and (b) PMA-PVDF/PEG nanofiber membranes.

Table 2. T_g, T_m, and degree of crystallinity of PMA-PVDF, and PMA-PVDF/PEG nanofiber membranes.

Sample	T_g [˚C]	T_m [˚C]	ΔH_m [J g^{-1}]	γ_c[%]
S1	-2	139.66	4.24	4.04
S2	-15	147.1	12.42	11.7
S3	-18	151.1	28.2	26.9
S4	-21	155.4	32.77	31.3
S5	-53	149.3	17.72	16.9
S6	-56	150	19.75	18.8
S7	-65.54	148.27	27.53	26.3

The miscibility of polymer/plasticizer system is usually determined from the glass transition temperature (T_g). The melting temperature depression is also an indicator of a miscible system. A

gradually decrease of T_g and slightly reduced of T_m with increase the PEG in PMA-PVDF/PEG blend is observed. Therefore, PEG is compatible with the PMA-PVDF blend[35] Compared with the electrospun nanofiber PMA-PVDF membrane with (χ_c %= 31.3), the electrospun blend samples in the presence of PEG showed lower crystallinity corresponding to the lower melting enthalpy which indicate that PEG act plasticization role for PMA-PVDF successfully but the degree of crystallinity of electrospun PMA-PVDF/PEG blend increased from 16.9% to 26.3% as the PEG wt% increased from 2 wt% to 8 wt%.

3.3. Morphological analysis

Fig. 3 shows the morphology of electrospun PMA-PVDF membranes with different wt% ratios (S1, S2, S3, and S4). For S1 membrane, the fibers are connected with each other forming a network structure due to the elastic nature of the PMA. Increasing the wt% of PVDF in the blend to 6 wt% (S2), the film has interconnected multifibrous layers with ultrafine narrow porous structure [36] and the average fiber diameter is 580 nm.

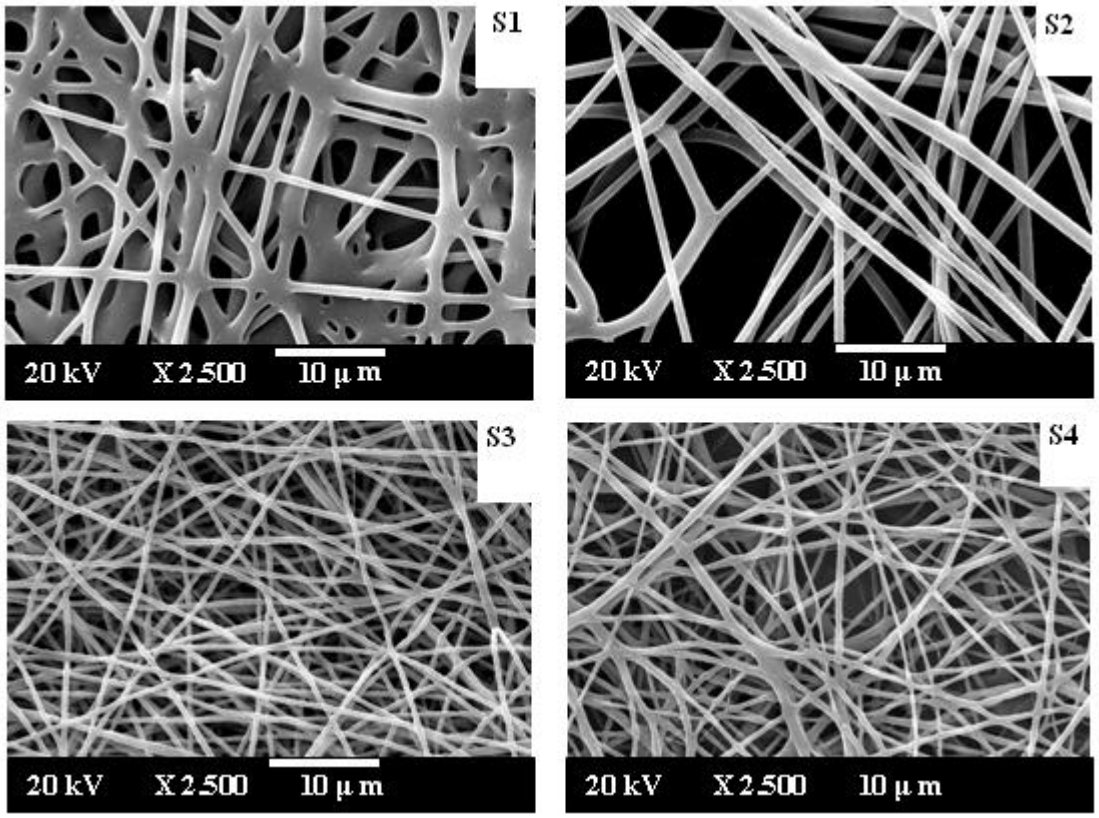

Figure 3. SEM images of electrospun PMA-PVDF nanofiber membranes with different weight ratios.

S3 sample has uniform fibers with average fiber diameter of 500 nm. The increased content of PVDF has been attributed to increasing dielectric constant of the medium for electrospinning. Electrospun jets are easily formed at the nozzle of the syringe for the composite solution, which caused the formation of fibers with lower diameter.[36] Increasing the ratio of PVDF in the blend to 7 wt%

(S4) led to slightly increase in the fibers diameter to 510 nm. In order to reduce the fibers diameter and improve the fibers quality, PEG with different wt% ratios is blended with the optimal PMA-PVDF weight ratio of (4:6 w/w) and electrospun. Fig. 3 shows the effect of addition of PEG with different wt ratios of 2, 4, and 8 (S5, S6, and S7, respectively). Electrospun S5 membrane has average fiber diameter of ~223 μm. The fibers are uniform, linear and interconnected. By increasing the wt% of PEG in the blend to 4 and 8 wt% (S6, and S7), the nanofibers diameter of S6 and S7 has an average fiber diameter of 250 and 370 nm with uniform and porous structure. It was found that, increasing the PEG wt% ratio, the fiber diameter is consequently increased due to increasing the viscosity of the solution.[37]

Generally, the presence of PEG in the blend leads to increase polarity of the medium for electrospinning. Electrospun jets are easily formed at the nozzle of the syringe for PMA-PVDF/PEG blend and cause the formation of fibers with lower diameter than the diameter of PMA-PVDF system. [36,38]

3.4. Electrolyte uptake

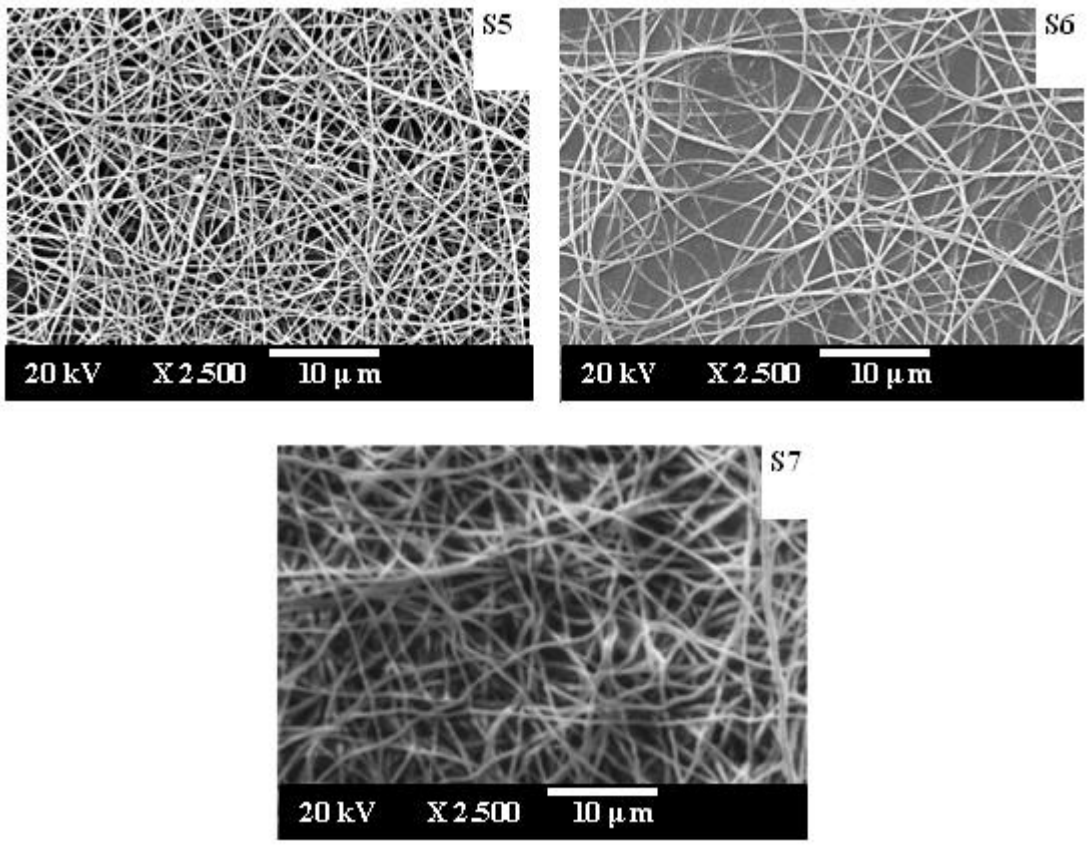

Figure 4. SEM images of electrospun PMA-PVDF/PEG nanofiber membranes with different weight ratios.

The polymer membrane with high porosity is suitable for incorporation of large amounts of liquid electrolyte and can attain high ionic conductivity at room temperature. All the prepared

membranes had good porosity due to their well-developed interstices as shown in Fig.s. 3 and 4 by the interwoven structure among nanofibers.[3,24] Table 3 presents a comparison of the electrolyte uptake of the nanofiber membranes as calculated from Equation 2.

The data was obtained by soaking the nanofiber membranes in the liquid electrolyte of 0.5 M LiI, 0.05 M I_2, and 0.5 M 4-*tert*-butylpyridine in 3-methoxyproponitrile for 1 h. Also, the results of porosity determination by n-butanol uptake method are calculated from Equation 3 and presented in Table 3. For PMA-PVDF membranes, the electrolyte uptake is increased steadily with the increase of PVDF wt% (S3) due to the high porosity of 76% and the pores are fully interconnected which increased the ability to uptake sufficient electrolyte solution in its pores.[17] For S4, the electrolyte uptake is decreased as a result of the decrease in the membrane porosity due to the enhencement in the average fiber diameter values (S4). For PMA-PVDF/PEG; the maximum absorption of the large quantities of liquid electrolyte by nanofiber membrane of S6 sample is obtained due to the high porosity of the membranes and the high amorphous content of the polymer.[24]

Table 3. Electrolyte uptake, porosity and the ionic conductivities of the nanofiber membranes.

Sample	Electrolyte uptake [%]	Porosity [%]	Ionic conductivity [S cm^{-1}]
S1	166.5	65.5	9×10^{-4}
S2	203	70	1.7×10^{-3}
S3	265	76	2.1×10^{-3}
S4	209.6	71	1.66×10^{-3}
S5	335	84	2.78×10^{-3}
S6	406.3	89	3.2×10^{-3}
S7	356.8	81	2.68×10^{-3}

3.5. Ionic conductivity

The ionic conductivities of the nanofiber membranes are measured at room temperature by the AC impedance method presented in Table 3 and the data are calculated from Equation 4. High porosity of the electrospun membrane and fully interconnectivity of macropores makes fast penetration of the liquid into the membrane resulting in an increase in AC ionic conductivity at room temperature.[24,39]

Fig. 5 shows the Nyquist plots of electrospun nanofiber membranes. The intercept on the real-axis exhibiting bulk resistance varies between 5 Ω for PMA to 1.9 Ω for PMA-PVDF (4:6 wt%), and 1 Ω for PMA-PVDF/PEG (4:6:4 wt%). The ionic of electrospun PMA-PVDF with 4:6 wt% (S4) has the highest ionic conductivity value of 2.1×10^{-3} S cm^{-1} because of interwoven structure introduced during electrospinning. In addition, the incorporation of PEG into the nanofiber membranes with 2 and 4 wt% improved the ionic conductivity from 2.78×10^{-3} S cm^{-1} to 3.2×10^{-3} S cm^{-1}. The enhancement of ionic conductivity in composite polymer electrolytes has been attributed mainly to the formation of efficient ion transport channels.[24]

3.6. Performance of quasi solid electrolyte DSSC cells

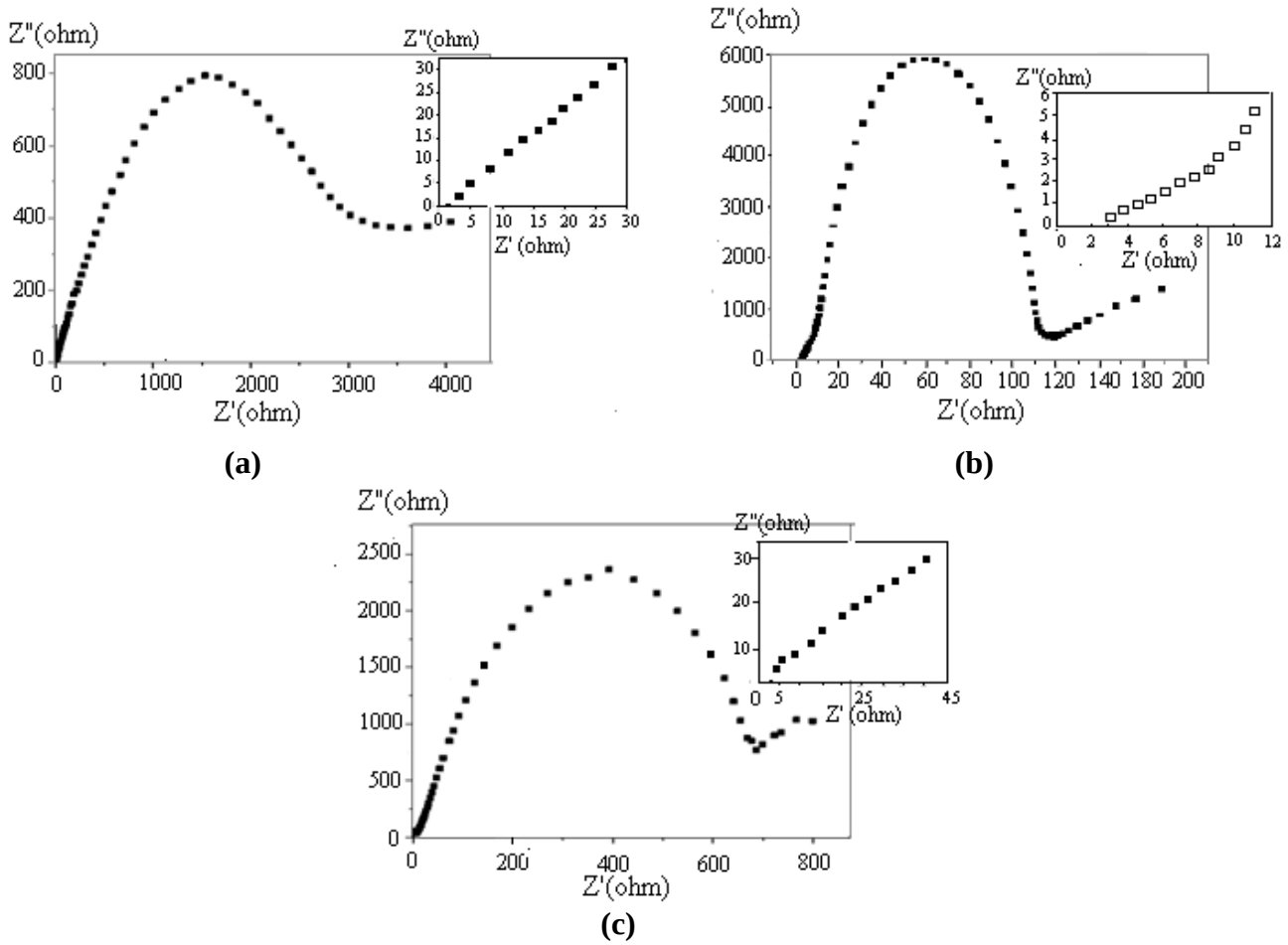

Figure 5. Nyquist plots of polymer electrolyte based on the nanofiber membranes (a) PMA, (b) PMA-PVDF(4:6 wt%)(S3), and (c) PMA-PVDF/PEG(4:6:4 wt%)(S6).

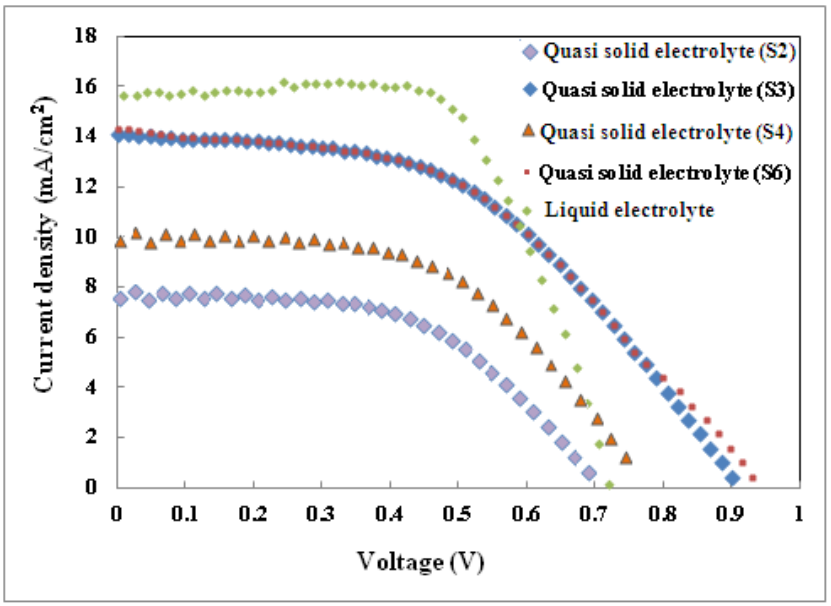

Figure 6. J–V curves of the DSSCs with electrospum membrane electrolyte (PMA-PVDF and PMA-PVDF/PEG), and liquid electrolyte.

The J-V curves of the DSSCs based on nanofiber membrane electrolyte (PMA-PVdF and PMA-PVDF/PEG) and liquid electrolyte at a light intensity of 100 mW cm^{-2} are shown in Fig. 6 and the photovoltaic parameters are summarized in Table 4.

For PMA-PVDF nanofiber membrane electrolyte; the maximum η of 6.6%, V_{oc} of 0.9 V, J_{sc} of 14.1 mA cm^{-2}, and FF of 0.52 are obtained using S3 membrane (4:6 wt% PMA-PVdF) which has the smallest average fiber diameter of 500 nm and the highest ionic conductivity of $2.1x10^{-3}$ S cm^{-1} compared with S2 and S4 membranes.

For PMA-PVDF/PEG nanofiber membrane electrolyte, It is noted that an enhanced η (7%), V_{oc} (0.93 V), and J_{sc} (17.22 mA cm^{-2}) values were observed, whereas the FF is remained the same. This may be attributed to the facility of electrolyte ions transfer through this nanofiber membrane [40] due to the high crystallinity, uniform nanofiber with average fiber diameter of 320 nm and high ionic conductivity.

Table 4. Photovoltaic characteristics[a] of DSSCs based on electrospun nanofiber membranes (PMA–PVDF and PMA-PVDF/PEG) and liquid electrolyte.

Electrolyte		V_{oc} (V)	J_{sc} (mA cm^{-2})	FF	η (%)
Quasi-solid electrolyte	PMA-PVDF (wt%)				
	S2	0.7	7.6	0.544	2.9
	S3	0.9	14.1	0.52	6.6
	S4	0.752	9.6	0.43	3.1
	PMA-PVDF/PEG (wt%)				
	S6	0.93	14.2	0.53	7
Liquid electrolyte		0.724	17.22	0.66	8.23

[a] All the devices are measured by solar simulator under illumination at AM 1.5 condition. The thickness of the electrospun PMA–PVDF and PMA–PVDF/PEG membranes nanofibers is 30 μm.

From the comparison between the photovoltaic parameters of DSSCs based on electrospun nanofiber membranes (PMA–PVDF and PMA-PVDF/PEG) and liquid electrolyte as in Table 1; it is observed that an enhancement in V_{oc} and reduced in J_{sc} in the case of quasi-solid-state DSSCs. When the electrospun membrane is used, it reduces the ionic motilities of the triiodide and iodide ions through the polymer membrane in the electrolyte solution.[17]

The decreased in the reduction rate constant of triiodide ion leads to increase V_{oc} according to the following Equation 7:[41]

$$V_{oc} = \left(\frac{KT}{e}\right) \ln\left(\frac{I_{inj}}{n_{cb}\ K_{et}(I_3^-)}\right) \qquad (7)$$

where I_{inj} is the flux of charge resulting from sensitized injection and n_{cb} is the concentration of electrons at the TiO_2 surface, k_{et} is the reduction rate constant and T is the cell absolute temperature. The enhanced V_{oc} values in the case of the DSSC with PMA-PVDF/PEG nanofiber membrane

compared to that in the DSSC with liquid electrolyte, the number of excited states of the dye molecules is reduced, which are involved in the electron injection process.[17] Also, PEG can interact with TiO_2 through Ti-O bonds and suppress back electron transfer from TiO_2 to I_3^- at the TiO_2/ electrolyte interface, which is beneficial to the improvement of the open-circuit voltage (V_{oc}).[42]

4. CONCLUSIONS

New quasi-solid state dye-sensitized solar cells based on membranes of PMA-PVDF and PMA-PVDF/PEG nanofiber electrolyte were fabricated. PMA/PVDF nanofiber membranes were prepared using different wt% in a mixture of acetone/DMF (6:4 v/v). The optimum weight ratio was 4:6 wt%, which exhibited average fiber diameter value of 500 nm and ionic conductivity of 2.1×10^{-3} S cm^{-1} at room temperature. Furthermore, the overall energy conversion efficiency of quasi solid state DSSC was 6.6 % at a light intensity of 100 mW cm^{-2}. The presence of PEG in PMA-PVDF membrane showed a decrease of the average fiber diameter to about 223 nm and increasing the ionic conductivity and the energy conversion efficiency into 3.2×10^{-3} S cm^{-1} and 7%, respectively. The fabricated membranes and consequently the resulted good efficiency are promising for scaling up this type of solar cells to large areas for the facile fabrication process and good homogeneity.

ACKNOWLEDGEMENT
This work has been done under the project funded by Science and Technology Development Fund (STDF), project ID:1414, " Quantum Dots Nanomaterials Dye Sensitized Solar Cells".

References

1. Y. Wu, W. H. Zhu, S. M. Zakeeruddin, M. Grätzel, *ACS Appl. Mater. Interfaces,* 7, 2015, 9307.
2. Z. Min, S. Qiong, Z. Mei, L. Yang, L. Qiuhong, D. Lifeng, *Applied Physics A,* 120, 2015, 595.
3. I. Chung, B. Lee, J. He, R. P. H. Chang, M. G. Kanatzidis, *Nature,* 485, 2012, 486.
4. X. Liu, W. Zhang, S. Uchida, L. Cai, B. Liu, S. Ramakrishna, *Adv. Mater.,* 22, 2010, E150.
5. M.-H. Jung, *Journal of Power Sources*, 268, 2014, 557.
6. U. Bach, D. Lupo, P. Comte, J. E. Moser, F. Weissortel, J. Salbeck, H. Spreitzer, M. Gratzel, *Nature,* 395, 1998, 583.
7. N. Cai, S.-J. Moon, L. Cevey-Ha, T. Moehl, R. Humphry-Baker, P. Wang, S. M. Zakeeruddin, M. Gratzel, *Nano Lett.,* 11, 2011, 1452.
8. A. Hagfeldt, G. Boschloo, L. C. Sun, L. Kloo, H. Pettersson, *Chem. Rev.,* 110, 2010, 6595.
9. A. K. Arof, M. Naeem, F. Hameed, W. J. M. J. S. R. Jayasundara, M. A. Careem, L. P. Teo, M. H. Buraidah, *Opt. Quantum Electron.,* 46, 2014, 143.
10. Z. Lan, J. Wu, D. Wang, S. Hao, J. Lin, Y. Huang, *Sol. Energy,* 80, 2006, 1483.
11. J. Wu, Z. Lan, D. Wang, S. Hao, J. Lin, Y. Wei, S. Yin, T. Sato, *J. Photochem. Photobiol. A Chem.,* 181, 2006, 333.
12. O. A. Ileperuma, G.R.A. Kumara, H.-S. Yang, K. Murakami, *J. Photochem. Photobiol. A Chem.,* 217, 2011, 308–312.
13. W. Xiang, Y. Fang, Y. Lin, S. Fang, *Electrochim. Acta,* 56, 2011, 1605–1610.
14. C.-W. Tu, K.-Y. Liu, A.-T. Chien, C.-H. Lee, K.-C. Ho, K.-F. Lin, *Eur. Polym. J.,* 44, 2008, 608.
15. T. Uyar, F. Besenbacher, *Polym.,* 49, 2008, 5336.

16. A. Formhals, U.S. Patent 1975504, 1934.
17. A.R. Sathiya Priya, A. Subramania, Y.-S. Jung, K.-J. Kim, *Langmuir*, 24, 2008, 9816.
18. M. Fathy, A. B. Kashyout, J. El Nady, Sh. Ebrahim, M. B. Soliman, *Alexandria Eng. J*, 2016, DOI:10.1016/j.aej.2016.03.019.
19. T. Ma, Z. Cui, Y. Wu, S. Qin, H. Wang, F. Yan, N. Han, J. Li, *J. Membr. Sci.*, 444, 2013, 213.
20. Y. Yang , J. Zhang , C. Zhou , S. Wu, S. Xu , W. Liu , H. Han , B. Chen , X. Z. *Zhao, J Phys Chem B.*, 112, 2008, 6594.
21. A. B. Kashyout**,** M. Fathy, M. Soliman, *Int. J. Photoenergy*, 2011, DOI 10.1155/2011/139374.
22. A. B. Kashyout, M. Soliman, M. Fathy, *Renewable Energy*, 35, 2010, 2914.
23. K Gao, X Hu, C Dai, T Yi, *Materials Science and Engineering: B*, 131,2006, 100.
24. Y.- J. Kim, C. H. Ahn, M. B. Lee, M. - S. Choi, *Mater. Chem. Phys.*, 127, 2011, 137.
25. P. Raghavan, X. Zhao, J.- K. Kim, J. Manuel, G. S. Chauhan, J. - H. Ahn, C. Nahb, *Electrochim. Acta*, 54, 2008, 228.
26. J. R. Kim, S. W. Choi, S. M. Jo, W. S. Lee, B. C. Kim, *J. Electrochem. Soc.* 152, 2005, A295.
27. Z. Tang, L. Qi, G. Gao, *Polym Adv Technol.* 21, 2010, 153–715.
28. R. Singh, N.A. Jadhav, S. Majumder, B. Bhattacharya, P.K. Singh, *Carbohydr. Polym.*, 91, 2013, 682.
29. W. Brostow, T. Datashvili, K. P. Hackenberg, e-Polym., 2008 no. 054.
30. W. Tang, T. Zhu, P. Zhou, W. Zhao, Q. Wang, G. Feng, H. Yuan, *J Mater Sci.* 46, 2011, 6656.
31. I. S. Elashmawi, N. A. Hakeem, *Polymer Engineering & Science* 48, 2008, 895.
32. K. Pandey, N. Asthana, M. M. Dwivedi, S. K. Chaturvedi, *J. Polym.* 2013 Article ID 752596, DOI 10.1155/2013/752596.
33. J. Gong, K. Sumathy, J. Liang, *Renewable Energy*, 39, 2012,419.
34. M. Tazaki, R. Wada, M. O. Abe,T. Homma, *Applied Polymer Science*, 65, 1997, 1517.
35. Y. Yoon, K. E. Park, S. J. Lee, W. H. Park, BioMed Res. Int. 2013, DOI 10.1155/2013/309048.
36. N. Wu, Q. Cao, X. Wang, X. Li, H. Deng, *Power Sources*,196, 2011, 8638.
37. K. Arayanarakul, N. Choktaweesap, D. Ahtong, C. Meechaisue, P. Supaphol, *Macromol Mater Eng.*, 291, 2006, 581.
38. D. Saikia, C.C. Han, Y.W. Chen-Yang, *Power Sources*, 185, 2008, 570.
39. J. Xi, X. Qiu, J. Li, X. Tang, W. Zhu, L. Chen, *Power Sources*, 157, 2006, 501.
40. W. S. Arsyad, Herman, Fitrilawati, R. Hidayat, *Advanced Materials Research*, 1112, 2015, 256.
41. M. K. Nazeeruddin, A. Kay, I. Rodicio, R. Humphry Baker, E. Miller, P. Liska, N. Vlachopoulus, M. Grätzel, *J. Am. Chem. Soc.* 115, 1993, 6382.
42. J. Shi, Sh. Peng, J. Pei, Y. Liang, F. Cheng, J. Chen, *Applied Materials & Interfaces*, 1, 2009, 944.